23rd ABCM International Congress of Mechanical Engineering
December 6-11, 2015, Rio de Janeiro, RJ, Brazil

EXPERIMENTAL AND NUMERICAL STUDIES OF VISCOELASTIC POLYMER SOLUTION FLOWS THROUGH CONSTRICTED MICRO CAPILLARY

Mario Caetano P. de Sá
Danmer Maza
Márcio S. Carvalho
PUC-Rio, Department of Mechanical Engineering, Rua Marquês de São Vicente, 225, Gávea, 22453-900 Rio de Janeiro, RJ, Brazil
paretomario@gmail.com; danmerm@gmail.com; msc@puc-rio.br

Abstract. *The injection of polymer solution is used as an Enhanced Oil Recovery method in many oil fields. The addition of polymer molecules to the injected water increases its viscosity, leading to a better mobility ratio between the oil and water phases and consequently larger volumes of produced oil. However, despite recent progress, the fundamental understanding on how elastic properties of a polymer solution improve oil recovery is still not complete. Because of the complexity of the flow, different mechanisms for residual oil mobilization have been proposed. The relative importance of each of these mechanisms is not clear.*
The geometry of a single pore throat resembles that of a constricted micro capillary. Here, we study numerically and experimentally the flow of viscoelastic solution in this geometry. The goal was to determine the pressure drop – flow rate relation as a function of geometry and rheological properties of the liquid.
The Oldroyd-B and FENE-CR constitutive equations that approximate viscoelastic behavior of polymer solutions were used, together with momentum and continuity equations, to model two-dimensional axisymmetric flow through micro capillaries. The equation system was solved with the Finite Element Method. The results show how the viscoelastic properties can affect the stress field in the liquid and the pressure drop – flow rate relation.
Experimental Results show that, above a certain flow rate, the pressure drop is not fully described by the viscous flow and elastic effects need to be taken into account. The reduced mobility of the water phase due to the extension of polymer molecules, as they flow through the converging-diverging channel, can be used to improve oil displacement in porous media.

Keywords: *Viscoelastic liquids; Extensional flow; Polymer solution; Finite element method*

1. INTRODUCTION

Viscoelastic capillary flow have practical applications in several industry segments. Polymer processing (Purnode and Crochet (1998)), coating industry (Romero et al. (2006)) and Enhanced Oil Recovery (EOR) (Afsharpoor et al. (2012); Zhang et al. (2010)). Nowadays, in the oil industry, several polymers such as hydrolyzed-polyacrylamide (HPAM), poly-ethylene oxide (PEO) and xanthan gum are used as viscosifying agents in solutions used in flooding mechanisms to improve oil recovery, in order to avoid well-known problems such as Saffman-Taylor instabilities (Avendano et al. (2013)) and as a consequence early water breakthrough in production wells. Applications of such technique in oilfields are reported since the 1960's, mostly on experimental works (Pye (1964) and Sandiford (1964)) that indicated this could be a cost-effective way to improve recovery on fields with a very wide range of oil and reservoirs characteristics.

Liquids used in EOR, in practice, are diluted polymer water solutions or colloidal suspensions. Depending on parameters such as molecular weight and concentration, polymer solutions can show a shear thinning or Boger fluid behavior. They can develop viscoelastic stresses when they are sheared or extended and both modes occur in porous media flow (Afsharpoor et al. (2012)). Operating parameters such as flow rate, maximum strain rate and temperature must be well defined to avoid solution thermos-mechanical degradation and as a consequence loss of sweep and displacement efficiency at reservoir scale (Al Hashmi et al. (2013)).

An ideal porous media can be modeled as a network of convergent/divergent channels, represented as pores and pore-throats (Zhang et al. (2010)). Due to the extensional flow present on the capillary model, normal stresses appears as a result of the stretching and alignment of polymer coils nearby the constriction. As mentioned in the literature (Afsharpoor et al. (2012); Tirtaatmadja and Sridhar (1995)), an increase of normal forces helps improving the pressure drop and mobilize trapped oil droplets, which would improve the global recovery factor.

Several constitutive models have been developed over the last decades in order to predict the viscoelastic behavior that dominate highly extensional flow of polymer solutions such as Oldroyd-B (Oldroyd (1950)) and FENE-CR

(Rallison and Chilcott (1988)). Some authors focus on the vortex growth prediction problem (Boger et al. (1992); Campo-Deaño et al. (2011); Purnode and Crochet (1998)), an others try to understand why the Enhanced Pressure Drop (EPD), defined as $EPD = \Delta P_{viscoelastic}/\Delta P_{viscous}$, observed experimentally is not represented by these models (Szabo et al., (1997); Binding et al. (2006); Walters et al. (2009); Tamaddon Jahromi et al. (2011)). Walters et al. (2009) suggest that Oldroyd-B model wouldn't predict better Boger fluids due to its intrinsic high dependency of the first normal stress difference (N1) on the shear rate. Introducing a factor "J", that turned the N1 dependency on shear rate, they observed EPD > 1 even for low Weissenberg numbers.

This paper presents a theoretical approach in the flow of diluted polymer solutions through a single pore model (a constricted capillary). The Oldroyd-B and FENE-CR constitutive equations that approximate viscoelastic behavior of polymer solutions were used, together with momentum and continuity equations, to model two-dimensional axisymmetric flow through micro capillaries. The equation system was solved with the Finite Element Method. The results shows the influence of the rheological parameters such as viscosity ratio, polymer relaxation time and flow rate on both constitutive models. Experimental Results show that, above a certain flow rate, the pressure drop is not fully described by the viscous flow and elastic effects need to be taken into account. The reduced mobility of the water phase due to the extension of polymer molecules, as they flow through the converging-diverging channel, can be used to improve oil displacement in porous media.

2. MATHEMATICAL FORMULATION

2.1 Geometric representation

Experimental results were obtained using glass micro-capillaries with constriction. In order to compare our first Newtonian predictions with experimental data, results conclude that a simple geometric representation (a symmetric model) the flow was not predicting well and was decided to improve the geometry. Based on a high-resolution microscopic photo (Figure 1a), we made a new representation using SolidWorks® software. With the new mesh, numerical discrepancy reduced from 11.5% to 6%.

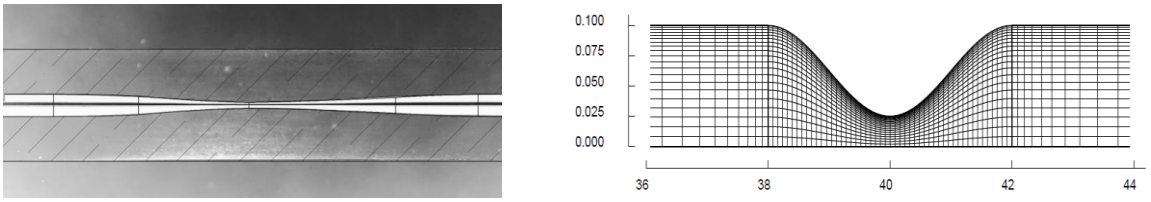

Figure 1. Left a, Microscopic photo of 200:50μm capillary. Right b, Sinusoidal Mesh for 200:50μm capillary

Despite the success achieved with Newtonian flows it was decided to use another geometric representation (Figure 1b), with a sinusoidal-based constriction. It works better for predictions using viscoelastic models to avoid issues like singularity points that could make the convergence harder.

2.2 Non-Newtonian problem formulation

Inertial effects were neglected (small Reynolds number). The flow was considered axisymmetric. The velocity field and pressure of the incompressible flow was defined by the two-dimensional (r, x) Navier-Stokes equations in steady-state coupled with a constitutive equations and subjected to the appropriate boundary conditions.

$$\nabla \cdot \mathrm{v} = 0 \qquad ; \qquad -\nabla p + \nabla \cdot \tau = 0 \tag{1,2}$$

In both models Oldroyd-B and FENE-CR, the total stress tensor τ is defined as the sum of the contributions from the solvent and the polymer molecules, $\tau = \tau_s + \tau_p$, the contribution from the solvent, a Newtonian liquid with viscosity ηs, is $\tau_s = 2\eta_s D$ and $D = 1/2(\nabla v + \nabla v^T)$, where D is the rate-of-deformation tensor, ∇v is the velocity gradient and $\nabla \mathrm{v}^{\mathrm{T}}$ is the transpose of ∇v. The polymer contribution (τ_p) for the stress tensor are described as constitutive models that are explained below.

The Oldroyd-B constitutive model, as well described in (Bird, et al., 1987), is a simple linear model, based on the dumbbell geometry. The model works well in shear flow, but its major drawback is in extensional flow where the polymer molecules can stretch infinitely and this is an unphysical behavior. The constitutive equation for Oldroyd-B is:

$$\tau_p + \lambda \tau_{p(1)} = \eta_p \dot{\gamma} \tag{3}$$

Where λ is the relaxation time (rheological parameter), η_p is the polymer viscosity and $\tau_{p(1)} \equiv v \cdot \nabla\tau_p - \nabla v^T \cdot \tau_p - \tau_p \cdot \nabla v$ is the upper convected derivative of the polymeric stress tensor. The material functions, extensional viscosity and the first normal stresses difference, in a steady shear free flow are given by the following expressions:

$$\eta_E = 3\eta_p \frac{1}{(1+\lambda\dot{\varepsilon})\cdot(1-2\lambda\dot{\varepsilon})} \quad ; \quad N_1 = 2\,\eta_S \lambda \dot{\gamma}^2 \tag{4,5}$$

Where η_s is the constant shear viscosity. The second normal stress difference is null (N_2=0).

The original Dumbbell with finitely extensible non-linear elastic (FENE) spring force behavior was first proposed by Warner Jr. (1972). It represents a linear behavior for small extensions and a finite extension in the limit of an infinite force. This feature eliminates the physical inconsistency that was intrinsic on the Oldroyd-B model.

In order to obtain a closed constitutive equation for the polymeric stress tensor, the FENE-P model , proposed by Peterlin and firstly used by Bird et al. (1980), substitutes the non-linear arrangement-dependent factor by an ensemble average term.

Rallison and Chilcott (1988), proposed a model evolution to compute numerically complex flows, known as FENE-CR. The model still uses Peterlin linearized approximation, but eliminates the shear rate dependence of the steady state viscosity in order to describe Boger fluids. Evolution equation for the FENE-CR model:

$$\tau_p + \frac{\lambda}{Z}\tau_{p(1)} - \frac{\lambda}{Z}\tau_p \frac{D(lnZ)}{Dt} = \eta_p \dot{\gamma} \quad ; \quad \mathrm{Z} = \frac{1+(\lambda/b\eta_p)tr(\tau_p)}{1-(3/b)} \tag{6,7}$$

Being *b* a dimensionless extensibility parameter, It is important no notice that when *b* goes to infinity the FENE models reduces to the Oldroyd-B equation. The material functions for the FENE-CR model are:

$$\eta_E = 3\eta_0 \frac{f^2}{(f+\lambda\dot{\varepsilon})\cdot(f-2\lambda\dot{\varepsilon})} \quad ; \quad N_1 = \frac{2\,\eta_0 \lambda \dot{\gamma}^2}{f^2} \tag{8,9}$$

and *f* is an extensional function, based on the conformation tensor A, $f\big(Tr(A)\big) = 1/[1 - Tr(A)/b^2]$, where Tr() is the trace operator.

The Weissenberg (Wi) number is a non-dimensional parameter used to measure the magnitude of a fluid's elasticity in a given flow, depending on the polymer relaxation time and the extensional rate imposed, $Wi = \lambda \cdot \dot{\varepsilon}$, where the extensional rate was defined as $\dot{\varepsilon} = \dot{v}_{(D_c)\cdot\Delta D/(D_{min}\cdot D_c)}$. So, $Wi = \lambda \cdot Q \cdot \Delta D/(A_c \cdot D_c \cdot D_{min})$, where λ is the polymer relaxation time. Q is the imposed flow rate, ΔD is the difference between the maximum diameter (D_{max}) and the minimum diameter (D_{min}) and D_c is the characteristic diameter, which is calculated through the Hagen-Poiseuille equation $Q = \Delta P \cdot \pi \cdot D^4/(128 \cdot L \cdot \mu)$. Polymer concentration is measured by the β parameter, which represents the ratio between elastic e viscous contributions, based on the viscosity ratio $\beta = \eta_s/(\eta_s + \eta_p)$.

3. SOLUTION METHOD

The momentum and mass conservation equations were solved with a Finite Element Method, where the velocity field, pressure and stress field were approximated with different basis functions. See more details in Romero (2003). Streamline Upwinding Petrov-Galerkin (SUPG) method was used to solve the polymeric stress equations due to their hyperbolic nature. The resulting set of nonlinear algebraic equations was solved simultaneously by Newton's method.

4. EXPERIMENTAL SETUP AND RESULTS

The experimental setup used in the analysis is sketched in Fig. 2a. It consisted of an appropriate Mariotte bottle (Maroto et al. 2002) used to feed the polymer solution at a constant inlet pressure through constricted quartz micro-capillary tubes. The flow rate is measure using a precision balance. The diameters of the glass capillary tube and the neck were equal to 200:50; 200:20 and 100:50 μm. The length of the capillaries was 8 cm and the position were the contraction and expansion occurs is in the middle of the length. Fig. 2b shows a photograph of the throat section of the capillary tube.

Three different concentration of PEO 8MM were prepared with deionized water (0.2%, 0.1%, and 0.05%). The rheological characterization was done using a rotational rheometer (Anton Paar Physica MCR301) and an extensional indexer (CABER), both shown in Fig. 3. The temperature was fixed at 24°C. The shear viscosity of PEO solution was measured using the cone-plate geometry (6cm, 1° cone angle). PEO solutions show a Boger fluid behavior at low concentration and low viscosity as shown also in Fig. 3a. The solutions in extensional response was probed with a capillary breakup extensional rheometer (CABER, Thermo Fisher Scientific). The elastic behavior of the PEO is much stronger at higher concentration, Fig. 3b.

Figure 4a shows a comparison of dimensionless pressure drop for different constriction ratios: 200:50, 200:20 and 100:50. For convenience, the pressure drops in this figure have been normalized with the viscous pressure drop. In all cases, at low Wi numbers the pressure drop of the PEO solution across the capillary are equal to the pressure drop observed for a viscous fluid with the same shear-rate viscosity ($\Delta P/\Delta P_N = 1$). As the Wi number is increased, the dimensionless pressure drop across the capillary with high constriction grows with Wi number until at a critical Wi = 50 is reached at which point the dimensionless pressure drop begins to saturate and the value of the dimensionless pressure drop increases. Figure 4b shows the flow of PEO at different concentration in micro-capillary of 100:50 where a weak extensional behavior is observed. The main conclusion here is in order to activate the elastic behavior of polymer solutions is necessary to have an appropriate constriction ratio.

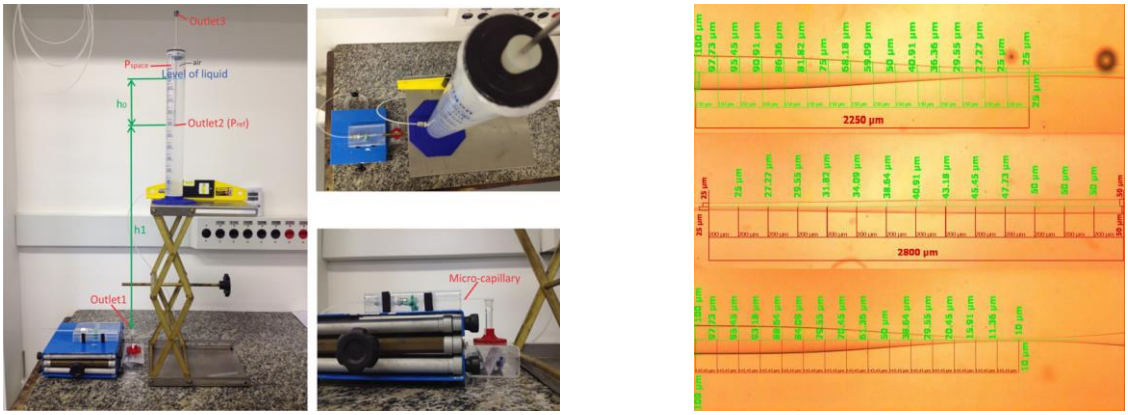

Figure 2. Left (a) Experimental set-up and Right (b) Different micro-capillary tube

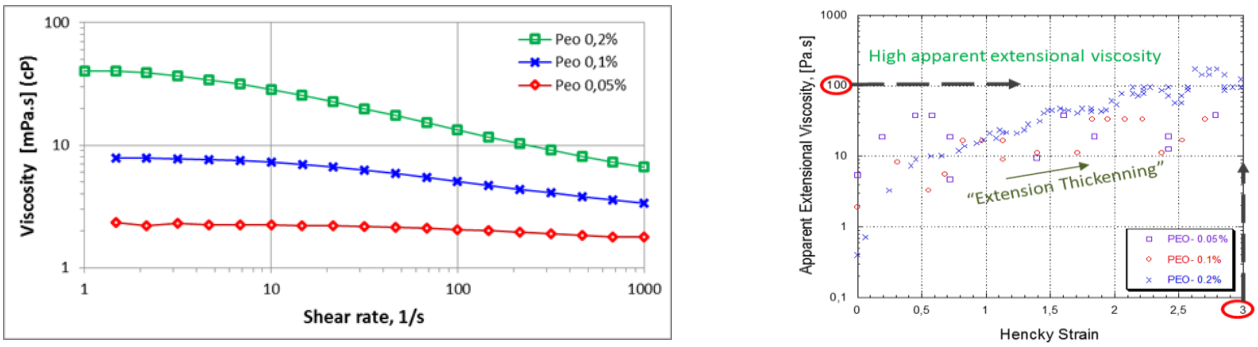

Figure 3. Rheological characterization of PEO at different concentration. Left(a), apparent viscosity vs shear rate. Right(b), apparent extensional viscosities vs Hencky strain.

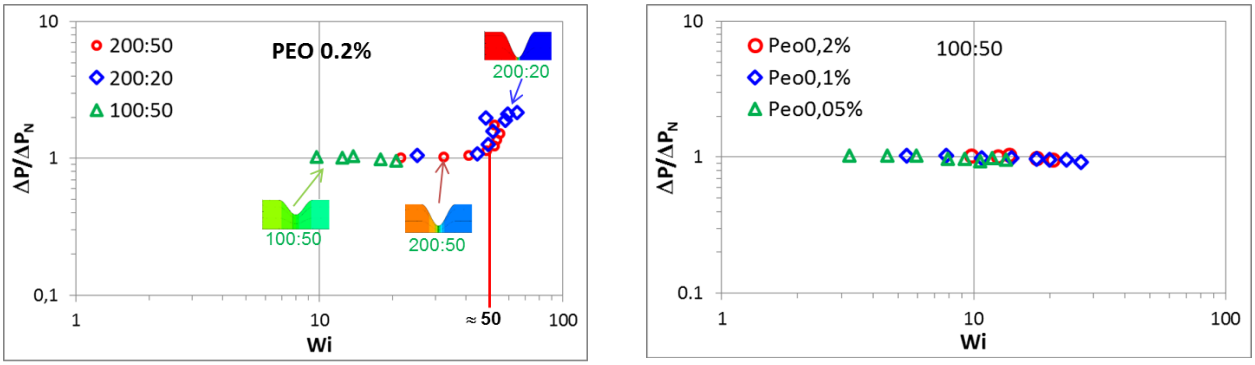

Figure 4. Dimensionless drop pressure ($\Delta P^* = \Delta P/\Delta P_N$) as a function Weissenberg number. Left) Flow of 0.2%PEO through different micro-channels. Right) Flow of PEO at different concentration in micro-capillary of 100:50

5. NUMERICAL RESULTS

The formulation and solution method used here were validated by Romero (2003), comparing the drag force resultant of a polymeric solution flow through a rigid cylinder with available results in the literature (Sun, et al., 1999).

Table 1 and 2 shows four different meshes that were used to verify mesh independency. The mesh that was used to obtain the present results (Mesh 3) is a 20x110 quadrangular mesh, which its elements were concentrated at the capillary wall. For this mesh, three different constriction ratios were used (2:1:2, 4:1:4 and 10:1:10). Mesh convergence test was made analyzing the tangent component of the polymeric stress along a streamline, near the capillary wall, with the flow of an Oldroyd-B fluid as shown in Fig. 5.

Table 1. Mesh properties for different number of elements

Meshes	Elem.	DoF (u, p, τ)	h Upwind
1 (Coarse)	400	8210	0,15
2 (Medium)	1050	20980	0,02
3 (Refined)	**2200**	**43370**	**0,018**
4 (Dense)	3975	78895	0,02

Table 2. Mesh convergence test for Wi = 3,81

Mesh	Max τ_{ptt}	% Variation
1 (Coarse)	4.82E+04	-
2 (Medium)	6.00E+04	19,7
4 (Dense)	6.56E+04	8,49
3 (Refined)	**6.89E+04**	**4,79**

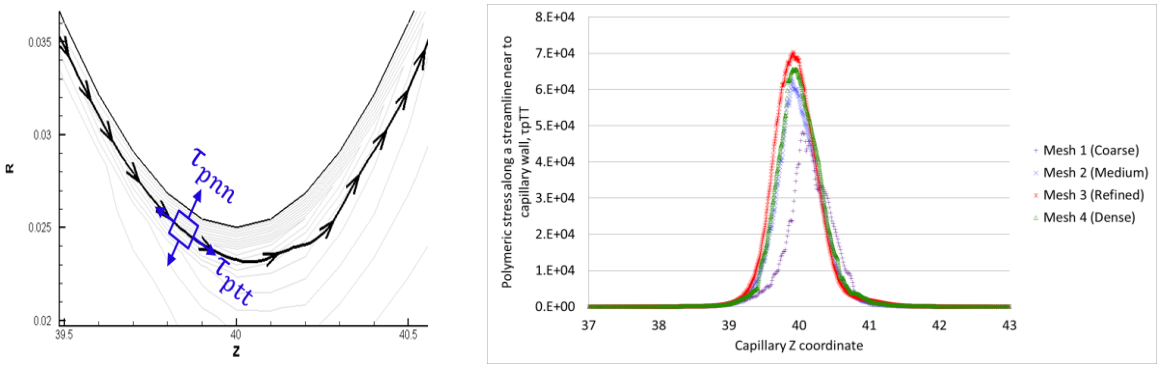

Figure 5. Mesh convergence test for Oldroyd-B fluid at Wi = 3.81. Left (a), Element on streamline near capillary wall. Right (b) Tangent polymeric stress component on streamline, τp_{tt}

Convergence was successfully achieved, as the percent variation of the analyzed tangent polymer stress component reduced from almost 20% to less than 5% between the medium and the refined mesh, compared to the coarse one. It's important to notice that the dense mesh, despite having more elements than the refined, had a worse result probably due to the fact that the elements were distributed uniformly and not concentrated at the top wall, where the stress is stronger.

5.1 Oldroyd-B

Figure 6 shows the EPD (ΔP*) as a function of Weissenberg (Wi) number for different Oldroyd-B fluids through a 200:50μm and 200:20μm respectively.

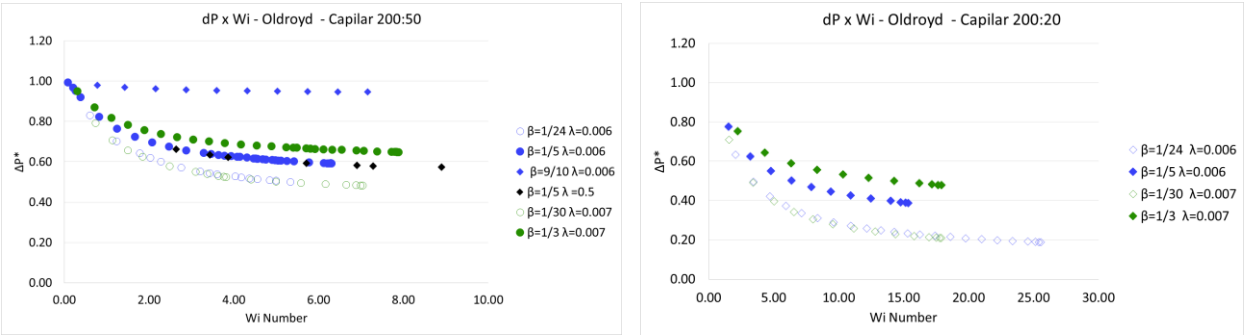

Figure 6. A: EPD (ΔP*) for Oldroyd-B model as a function of Wi number. Left (a) 200:50μm, Right (b) 200:20μm

As seen in previous works, the Oldroyd-B model reduces the pressure drop along the capillary, leading to an EPD < 1 situation. It is clear that increasing polymer contribution (reducing β) leads to a stronger reduction in pressure drop. Relaxation time doesn't seems to have a strong role on this relationship, as for β=1/5 both λ=0,006 and λ=0,5 have the same trend. Constriction ratio has a strong influence on it, for 2:1:2 constriction, EPD is always between 0.9 and 1.0, while for 4:1:4 it reaches a plateau of EPD=0.5 for β=1/24 and β=1/30 and, ultimately, reaches EPD<0.2 for the 10:1:10 constriction. High values of relaxation time leads to early loss of convergence. Observing Figure 7 it is clear that the

boundary layer is a mandatory agent in convergence, as the polymeric stress gradient is too strong near the constriction wall.

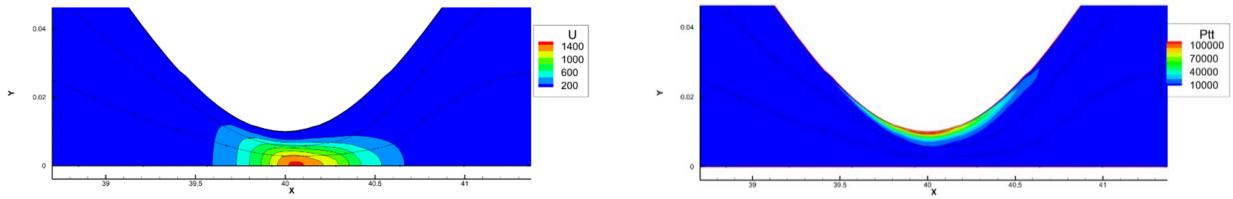

Figure 7. Oldroyd-B (β=1/24, λ=0,006) 200:20μm, Wi=25,58. Left (a) U velocity component. Right (b) Tangent polymeric stress component, τp_{tt}

5.2 FENE-CR

The first thing we analyzed on the FENE-CR model is the contribution of the finite extensibility parameter, *b*, on polymeric stress. As seen in 2.2, this parameter represents the length of polymer coils and when *b* is minimum, the polymer does not stretch at all and when *b* is maximum, the coils can be infinitely extensible, recovering the Oldroyd-B behavior.

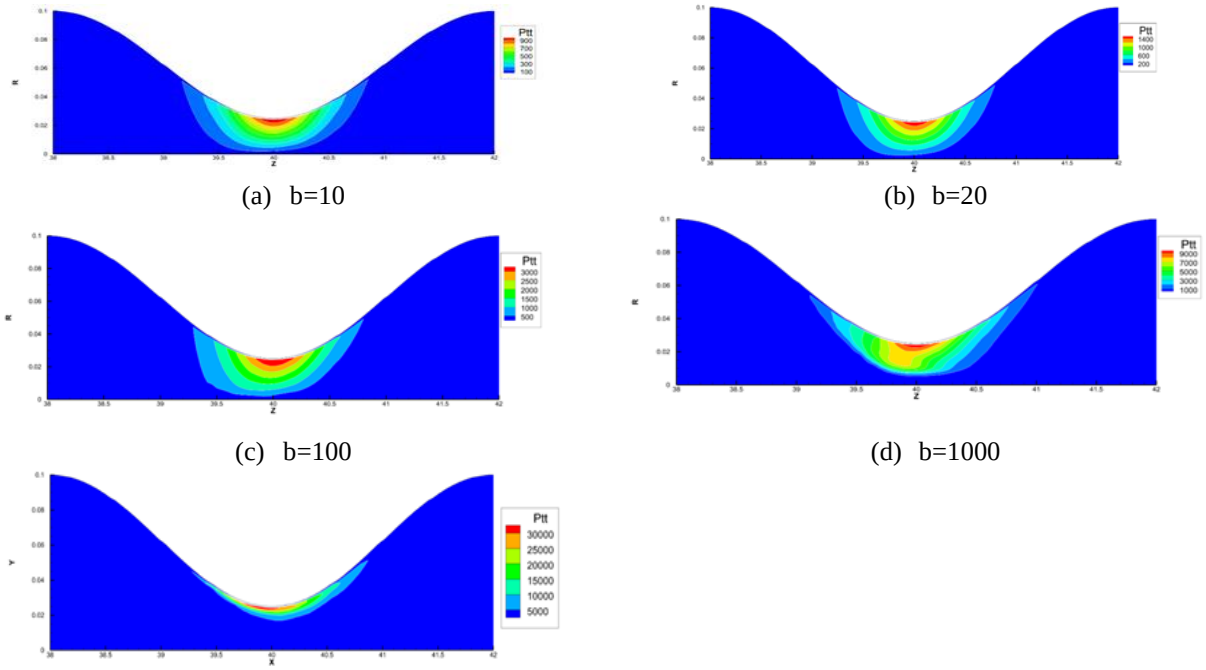

(a) b=10 (b) b=20

(c) b=100 (d) b=1000

(e) $b=10^5$

Figure 8. FENE-CR (β=1/5, λ=0,006) 200:50μm capillary Wi=6,4 - Tangent polymeric stress component, τp_{tt}

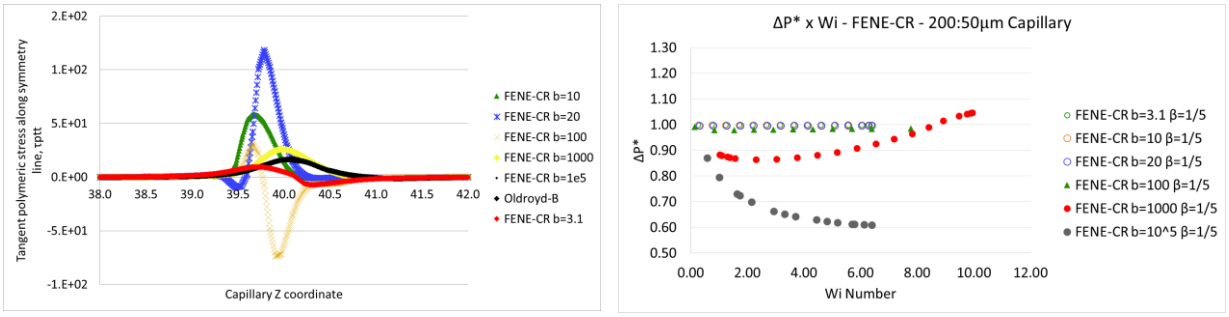

Figure 9. FENE-CR – Influence of b parameter. Left (a) Tangent polymeric stress component on symmetry line, τp_{tt}e, Right (b) EPD (ΔP*) x Wi

Figure 8 shows that the boundary layer problem also occurs for FENE-CR model, when high values of the extensibility parameter are used, i.e. when recovering Oldroyd-B model. Figure 9a shows the tangent polymeric stress

component calculated at the capillary symmetry line. Stress grows from minimum (b=3.1) to maximum (b=20) and then starts to decrease, as the boundary layer becomes thinner and so the high stress region becomes each time closer to the wall and further from the symmetry line. When b=10^5 the Oldroyd-B stress prediction is recovered.

6. FINAL REMARKS

Two different fluid constitutive models were implemented in a Navier-Stokes finite element method solver, in order to describe the flow of diluted polymer solutions through a constricted micro-capillary. The influence of rheological parameters and flow characteristics must be analyzed in each model in order to understand. On Figure 10 the pressure drop and flow rate relationship is compared for the three models studied on this work. It is clear that the 2:1:2 constriction doesn't create sufficient extensional rate to activate the polymer chains and so the three models have the same trend. For the 4:1:4 and 10:1:10 constriction ratios, different behaviors are seen. On both constrictions the Oldroyd-B leads to a reduction on the pressure drop, being stronger on the 10:1:10. The FENE-CR shows an interesting trend of EPD (ΔP^*)>1 for high flow rates on the 4:1:4 constriction, but, this trend could not be reproduced for the 10:1:10 capillary.

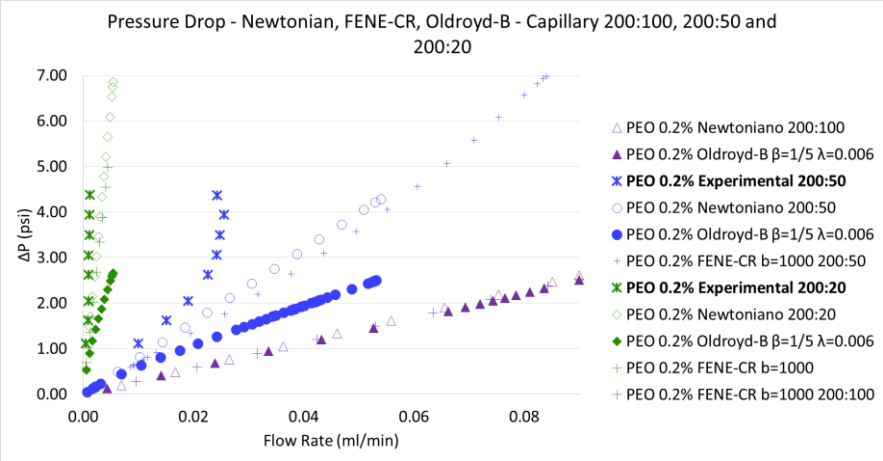

Figure 10. Newtonian, Oldroyd-B and FENE-CR Flow Rate x Pressure Drop predictions

Based on the previous results, numerical analysis of diluted polymeric solutions through constricted micro capillaries is influenced by:

The constitutive model used, and it's material functions: The Oldroyd-B model has limits of convergence to low Weissenberg numbers due to the high polymeric tension gradient on the capillary throat, leading to a boundary layer classic problem. As reported by recent studies (Tamaddon Jahromi, et al., 2011; Walters, et al., 2009), the Oldroyd-B model fails to predict the enhanced pressure drop due to its too strong first normal stress difference dependency on shear rate. The FENE-CR, when using a well calibrated "b" value, it stabilizes the pressure drop losses and it achieved EPD (ΔP^*) > 1 for the 4:1:4 constriction for b=1000. Convergence was limited and could not reproduce results for higher values of relaxation time, λ. While using lower values for b, were able to achieve high Wi numbers, but, without no gain in EPD.

Relaxation Time: For the Oldroyd-B model, an increase in λ leads to an aggressive increase of the polymeric stress gradient, and therefore the boundary layer issue disturbs convergence for higher flow rates. For the FENE-CR model, when using low values for b, it's possible to achieve convergence for satisfactory relaxation times and to observe deformations on the velocity fields due to the dominant elastic forces.

Viscosity Ratio: On the Oldroyd-B model, a reduction on β strengthen the undesired reduction on pressure drop, due to the increase of the polymeric contribution on tension. On the FENE-CR this influence was inconclusive, since the results were unstable for the studied case. Aguayo et al. (2008) reported better results with a high viscosity ratio (β=0.9). But, for this values, it couldn't achieve convergence for useful Wi numbers.

Constriction Ratio: For the Oldroyd-B model is clear that the increase on the constriction ratio leads to a stronger participation of the polymer properties. Drop of half ΔP^* was observed changing constriction ratio from 4:1:4 to 10:1:10. For the FENE-CR, apparently, the constriction ratio doesn't play a major role on the flow properties.

7. ACKNOWLEDGMENTS

The authors would like to thank Statoil and the Brazilian National Agency of Petroleum, Natural Gas and Biofuels (ANP) for the financial support.

8. REFERENCES

Afsharpoor, Ali, Balhoff, Matthew T., Bonnecaze, Roger, and Huh, Chun. , 2012. "CFD modeling of the effect of polymer elasticity on residual oil saturation at the pore-scale". *Journal of Petroleum Science and Engineering*, Vol. *94-95*, pp. 79–88.

Aguayo, J.P., Tamaddon-Jahromi, H.R., and Webster, M.F. , 2008. "Excess pressure-drop estimation in contraction and expansion flows for constant shear-viscosity, extension strain-hardening fluids". *Journal of Non-Newtonian Fluid Mechanics*, Vol. *153*, pp. 157–176.

aven, a.R., Al Maamari, R.S., Al Shabibi, I.S., Mansoor, a.M., Zaitoun, a., and Al Sharji, H.H. , 2013. "Rheology and mechanical degradation of high-molecular-weight partially hydrolyzed polyacrylamide during flow through capillaries". *Journal of Petroleum Science and Engineering*, Vol. *105*, pp. 100–106.

bin, J, Pannacci, N, Herzhaft, B, Gateau, P, and Coussot, P. , 2013. "Enhanced displacement of a liquid pushed by a viscoelastic fluid.". *Journal of Colloid and Interface Science*, Vol. *410*, pp. 172–80.

Binding, D.M., Phillips, P.M., and Phillips, T.N. , 2006. "Contraction/expansion flows: The pressure drop and related issues". *Journal of Non-Newtonian Fluid Mechanics*, Vol. *137*, pp. 31–38.

Bird, R B, Armstrong, R C, and Hassager, O. , 1987. "Dynamics of polymeric liquids - Vol 2 - Kinetic Theory".

Bird, R B, Dotson, P J, and Johnson, N L. , 1980. "Polymer solution rheology based on a finitely extensible bead-spring chain model". *Journal of Non-Newtonian Fluid Mechanics*, Vol. *7*, pp. 213–235.

Boger, D V, Crochet, M J, and Keiller, R A. , 1992. "On viscoelastic flows through abrupt contractions". *Journal of Non-Newtonian Fluid Mechanics*, Vol. *44*, pp. 267–279.

Campo-Deaño, Laura, Galindo-Rosales, Francisco J., Pinho, Fernando T., Alves, Manuel a., and Oliveira, Mónica S.N. , 2011. "Flow of low viscosity Boger fluids through a microfluidic hyperbolic contraction". *Journal of Non-Newtonian Fluid Mechanics*, Vol. *166*, pp. 1286–1296.

Romero, O.J., 2003. "*Limite de vazao minima para processos de revestimento por extrusao de solucoes polimericas.*". Pontifícia Universidade Católica do Rio de Janeiro.

Oldroyd, J.G. , 1950. "On the Formulation of Rheological Equations of State". *Proceedings of the Royal Society of London*, pp. 523–541.

Purnode, B and Crochet, M J. , 1998. "Polymer solution characterization with the FENE-P model". *Journal of Non-Newtonian Fluid Mechanics*, Vol. *77*, pp. 1–20.

Pye, David. , 1964. "Improved Secondary Recovery by Control of Water Mobility". *Journal of Petroleum Technology*, Vol. *16*, pp. 911–916.

Rallison, J M and Chilcott, M D. , 1988. "Creeping flow of dilute polymer solutions past cylinders and spheres". *Journal of Non-Newtonian Fluid Mechanics*, Vol. *29*, pp. 381–432.

Romero, O.J., Scriven, L.E., and Carvalho, M.S. , 2006. "Slot coating of mildly viscoelastic liquids". *Journal of Non-Newtonian Fluid Mechanics*, Vol. *138*, pp. 63–75.

Sandiford, B.B. , 1964. "Laboratory and Field Studies of Water Floods Using Polymer Solutions to Increase Oil Recoveries". *Journal of Petroleum Technology*, Vol. *16*.

Sun, J., Smith, M.D., Armstrong, R.C., and Brown, R.a. , 1999. "Finite element method for viscoelastic flows based on the discrete adaptive viscoelastic stress splitting and the discontinuous Galerkin method: DAVSS-G/DG". *Journal of Non-Newtonian Fluid Mechanics*, Vol. *86*, pp. 281–307.

Szabo, P., Rallison, J.M., and Hinch, E.J. , 1997. "Start-up of flow of a FENE-fluid through a 4:1:4 constriction in a tube". *Journal of Non-Newtonian Fluid Mechanics*, Vol. *72*, pp. 73–86.

Tamaddon Jahromi, H. R., Webster, M. F., and Williams, P. R. , 2011. "Excess pressure drop and drag calculations for strain-hardening fluids with mild shear-thinning: Contraction and falling sphere problems". *Journal of Non-Newtonian Fluid Mechanics*, Vol. *166*, pp. 939–950.

Tirtaatmadja, V. and Sridhar, T. , 1995. "Comparison of constitutive equations for polymer solutions in uniaxial extension". *Journal of Rheology*, Vol. *39*, pp. 1133.

Walters, K., Webster, M.F., and Tamaddon-Jahromi, H.R. , 2009. "The numerical simulation of some contraction flows of highly elastic liquids and their impact on the relevance of the Couette correction in extensional rheology". *Chemical Engineering Science*, Vol. *64*, pp. 4632–4639.

Warner Jr., Harold R. , 1972. "Kinetic theory and rheology of dilute suspensions of finitely extendible dumbbells". *Industrial & Engineering Chemistry Fundamentals*, Vol. *1*, pp. 379–387.

Zhang, Zhen, Li, Jiachun, and Zhou, Jifu. , 2010. "Microscopic Roles of “Viscoelasticity” in HPMA polymer flooding for EOR". *Transport in Porous Media*, Vol. *86*, pp. 199–214.

9. RESPONSIBILITY NOTICE

The authors are the only responsible for the printed material included in this paper.